Biochimica et Biophysica Acta 1818 (2012) 1764–1776

Contents lists available at SciVerse ScienceDirect

Biochimica et Biophysica Acta

journal homepage: www.elsevier.com/locate/bbamem

Lipid shape is a key factor for membrane interactions of amphipathic helical peptides

Erik Strandberg [a], Deniz Tiltak [b], Sebastian Ehni [a], Parvesh Wadhwani [a], Anne S. Ulrich [a,b,*]

[a] Karlsruhe Institute for Technology (KIT), Institute for Biolog
[b] KIT, Institute of Organic Chemistry and CFN, Fritz-Haber-W

ARTICLE INFO

Article history:
Received 24 November 2011
Received in revised form 22 February 2012
Accepted 27 February 2012
Available online 5 March 2012

Keywords:
Membrane-active amphipathic alpha-helical antimicrobial peptide
MSI-103 $[KIAGKIA]_3$-NH_2
Helix alignment and dynamics
Solid-state ^{2}H-NMR
Spontaneous bilayer curvature
Lipid shape concept

ABSTRACT

The membrane alignment of the amphiphilic α-helical model peptide MSI-103 (sequence $[KIAGKIA]_3$-NH_2) was examined by solid state ^{2}H-NMR in different lipid systems by systematically varying the acyl chain length and degree of saturation, the lipid head group type, and the peptide-to-lipid molar ratio. In liquid crystalline phosphatidylcholine (PC) lipids with saturated chains, the amphiphilic helix changes its orientation from a surface-bound "S-state" to a tilted "T-state" with increasing peptide concentration. In PC lipids with unsaturated chains, on the other hand, the S-state is found throughout all concentrations. Using phosphatidylethanolamine lipids with a small head group or by addition of lyso-lipids with only one acyl chain, the spontaneous curvature of the bilayer was purposefully changed. In the first case with a negative curvature only the S-state was found, whereas in systems with a positive curvature the peptide preferred the obliquely immersed T-state at high concentration. The orientation of MSI-103 thus correlates very well with the shape of the lipid molecules constituting the membrane. Lipid charge, on the other hand, was found to affect only the initial electrostatic attraction to the membrane surface but not the alignment preferences. In bilayers that are "sealed" with 20% cholesterol, MSI-103 cannot bind in a well-oriented manner and forms immobilized aggregates instead. We conclude that the curvature properties of a membrane are a key factor in the interactions of amphiphilic helical peptides in general, whose re-alignment and immersion preferences may thus be inferred in a straightforward manner from the lipid-shape concept.

1. Introduction

Membrane-active peptides are remarkable biological agents, as they tend to operate by physical principles as opposed to specific molecular recognition. Antimicrobial peptides (AMPs), cell-penetrating carriers, and fusogenic sequences are all known to perturb cellular membranes in order to carry out their respective function [1]. The surface charge and lipid composition of the target cell are generally accepted as the main factors that determine selectivity. For example, AMPs have to attack specifically bacterial membranes and need to avoid the membranes of eukaryotic host cells [2–4]. However, there exist no general rules to understand and predict the interactions of such peptides with any particular type of membrane system. That is because most peptides exhibit a complex range of interchanging conformations, membrane alignments, oligomeric states, and dynamic properties. To be able to systematically assess the effect of different lipid environments, the detailed behavior of a peptide has to be fully and comprehensively characterized first. Solid-state NMR is the method of choice for analyzing membrane-bound peptides in lipid bilayers [5–7], and even in native biomembranes [8,9]. ^{2}H-, ^{15}N-, and ^{19}F-NMR have been used to characterize many representative types of selectively labeled peptides in macroscopically oriented samples [6,7,10–18]. For example, the amphiphilic α-helical PGLa [19–21] and the designer analogue MSI-103 [22] have been thoroughly studied by ^{2}H-NMR, and PGLa [23,24]. MSI-103 [22], MAP [25], alamethicin [26], the cyclic β-pleated gramicidin S [27,28], as well as the fusion peptides FP23 [29] and B18 [30] have also been investigated by ^{19}F-NMR. In all of these systems several distinct structures were observed, suggesting that the peptides undergo functionally relevant changes in their conformation and/or membrane alignment [31]. Such changes need to be carefully monitored when comparing a peptide in different lipid systems in an attempt to find common features that may explain its membrane interactions and mechanism.

Abbreviations: AMP, antimicrobial peptide; CHOL, Cholesterol; DLPC, 1,2-dilauroyl-*sn*-glycero-3-phosphatidylcholine; DMPC, 1,2-dimyristoyl-*sn*-glycero-3-phosphatidylcholine; DMPG, 1,2-dimyristoyl-*sn*-glycero-3-phosphatidylglycerol; DMoPC, 1,2-dimyristoleoyl-*sn*-glycero-3-phosphatidylcholine; DOPC, 1,2-dioleoyl-*sn*-glycero-3-phosphatidylcholine; I-state, inserted state; L_α phase, liquid crystalline lamellar phase; Lyso-OPC, 1-oleoyl-2-hydroxy-*sn*-glycero-3-phosphatidylglycerol; MLV, multi-lamellar vesicle; OCD, oriented circular dichroism; PC, phosphatidylcholine; PE, phosphatidylethanolamine; PG, phosphatidylglycerol; P/L, peptide-to-lipid molar ratio; P/L*, threshold P/L value for peptide reorientation; POPC, 1-palmitoyl-2-oleoyl-*sn*-glycero-3-phosphatidylcholine; POPE, 1-palmitoyl-2-oleoyl-*sn*-glycero-3-phosphatidylethanolamine; POPG, 1-palmitoyl-2-oleoyl-*sn*-glycero-3-phosphatidylglycerol; R_0, radius of spontaneous curvature; ρ, azimuthal rotation angle; rmsd, root mean square deviation; σ_ρ, standard deviation of Gaussian distribution of azimuthal rotation angles; σ_τ, standard deviation of Gaussian distribution of tilt angles; S_{mol}, molecular order parameter; S-state, surface-aligned state; τ, tilt angle; T_m, gel to liquid crystalline phase transition temperature; T-state, tilted state

* Corresponding author at: Karlsruhe Institute for Technology (KIT), Institute of Organic Chemistry and CFN, Fritz-Haber-Weg 6, 76131 Karlsruhe, Germany. Tel.: +49 721 608 43912; fax: +49 721 608 44823.
E-mail address: anne.ulrich@kit.edu (A.S. Ulrich).

0005-2736
doi:10.1016/j.bbamem.2012.02.027

The natural antibiotic PGLa from the skin of *Xenopus laevis* was extensively characterized in uncharged DMPC and in anionic DMPC/DMPG lipid mixtures. The cationic peptide is unstructured in aqueous solution [32], but it gets electrostatically attracted to negatively charged vesicles where it folds as an α-helix [24,32]. It is also well folded in pure DMPC when reconstituted in a macroscopically oriented NMR sample without excess water (i.e. at 96% relative humidity). At low peptide-to-lipid ratios (P/L) (1:200 or lower) the helix axis of PGLa is aligned parallel to the membrane surface in the so-called "surface state" or S-state. Here, the tilt angle τ (defined as the angle between the helical axis and the bilayer normal) is close to 90°. The observed azimuthal rotation angle ρ places all charged side chains toward the aqueous layer, as expected from the amphiphilic character of this molecule. At higher peptide concentrations, P/L = 1:50 or higher, the helix inserts into the membrane with an oblique tilt angle of about 125° in the "tilted state" or T-state [19,23]. The threshold concentration between S- and T-states was found to be around P/L = 1:100 for PGLa in DMPC [20,33]. When PGLa was mixed 1:1 with magainin 2, a synergistic AMP from the same frog, it flipped into an "inserted" or I-state, suggesting that the two peptides together can form stable transmembrane pores [21]. The same upright orientation was observed when PGLa alone was embedded in the gel-phase of DMPC below the acyl chain melting temperature [34].

These re-alignment transitions of PGLa and other amphiphilic peptides clearly depend on multiple factors, such as peptide concentration, lipid composition, temperature, and degree of hydration. Among these factors, the lipid composition is one of the most important parameters explored in many biophysical studies of membrane-active peptides. However, there are hardly any reports in which the lipid characteristics have been systematically varied, while at the same time paying careful attention to the versatile structural responses of the peptide discussed above. Unfortunately, it would also be rather ambiguous to compare any existing data from different series of experiments in the literature, when carried out by different groups or under slightly different conditions. Therefore, we present here a comprehensive study on the effect of lipid composition on one representative peptide, using equivalent types of samples under reproducible conditions.

As an amphiphilic α-helical model peptide we selected MSI-103, a designer-made antibiotic based on the primary sequence of PGLa [35,36]. It has a pronounced antimicrobial activity and low hemolytic side effects, thus superseding even the natural PGLa in its therapeutic index [35,37]. We have recently compared its orientational behavior with that of PGLa using ^{2}H- and ^{19}F-NMR [22]. Both molecules were found to behave very similarly when examined in DMPC and DMPC/DMPG bilayers at P/L ratios from 1:800 to 1:20. At very low peptide concentration (P/L = 1:400 or lower), MSI-103 assumes a surface-bound S-state, which flips into the T-state at higher P/L. Its threshold concentration is about P/L = 1:200, lower than for PGLa [33], but the corresponding angles τ and ρ are equivalent for the two peptides in both alignment states [22]. In the present study, we chose MSI-103 because of this low re-alignment threshold, as the tendency to flip can be easily recognized at convenient P/L ratios. Another advantage is its regular repetitive sequence, which can be conveniently labeled with Ala-d_3 in many non-perturbing positions (Ala3, Ala7, Ala10, Ala14, Ala17, and Ala21) along the entire molecule. We did not label the outermost residues Ala3 and Ala21 at the termini, as they could be affected by unraveling of the α-helix. Instead, additional labels were included at positions Ile9, Gly11 and Ile13, such that the central stretch of the helix can be monitored contiguously over a total of 7 selective Ala-d_3 substitutions (see Table 1). In the following analysis of MSI-103 in over 15 different types of lipids and mixtures thereof (components listed in Table 2), more than 100 labeled samples were individually prepared and measured, often under several different conditions, to obtain a comprehensive overview of the peptide's alignment preferences.

So far, MSI-103 had been studied only in DMPC at different concentrations, and in DMPC/DMPG, in order to address the role of lipid charge.

Table 1
Amino acid sequences of the peptides used.

Peptide	Labeled position	Sequence
MSI-103	None	KIAGKIAKIAGKIAKIAGKIA-NH_2
MSI-103-A7	Ala7	KIAGKI-Ala-d_3-KIAGKIAKIAGKIA-NH_2
MSI-103-I9	Ile9	KIAGKIAK-Ala-d_3-AGKIAKIAGKIA-NH_2
MSI-103-A10	Ala10	KIAGKIAKI-Ala-d_3-GKIAKIAGKIA-NH_2
MSI-103-G11	Gly11	KIAGKIAKIA-Ala-d_3-KIAKIAGKIA-NH_2
MSI-103-I13	Ile13	KIAGKIAKIAGK-Ala-d_3-AKIAGKIA-NH_2
MSI-103-A14	Ala14	KIAGKIAKIAGKI-Ala-d_3-KIAGKIA-NH_2
MSI-103-A17	Ala17	KIAGKIAKIAGKIAKI-Ala-d_3-GKIA-NH_2

The presence of DMPG was found to have no effect on the re-alignment threshold, once the peptide was attracted to the membrane surface either electrostatically or by limited hydration conditions in oriented samples [20,22]. In the present study, a wide range of lipid systems are investigated with different acyl chains and head groups. Bacterial membranes are imitated by a high proportion of charged PG lipids and non-lamellar PE lipids, while eukaryotic plasma membranes are predominantly uncharged and rich in cholesterol [38]. Another factor of interest is the hydrophobic thickness of the lipid bilayer, as this parameter has not yet been examined for amphipathic peptides. In the case of transmembrane helices it has been shown by ^{15}N-NMR that Vpu from HIV-1 adjusts its tilt angle to compensate for the hydrophobic bilayer thickness [39,40]. A similar adjustment of helix orientation as a function of mismatch has also been described by ^{2}H-NMR for the WALP family of transmembrane peptides [41–44]. Therefore, under conditions where MSI-103 and PGLa assume an obliquely tilted orientation in one monolayer, or when they get fully inserted as a membrane-spanning complex, it would be interesting to find out whether the precise tilt angle varies with the hydrophobic bilayer thickness.

2. Materials and methods

2.1. Lipids

All lipids were purchased from Avanti Polar Lipids (Alabaster, AL, USA) and used without further purification. These lipids and some

Table 2
Lipids used.

Lipid	Full name	Acyl chains	Length[a] (Å)	T_m[b] (°C) [Ref.]
DLPC	1,2-Dilauroyl-*sn*-glycero-3-phosphatidylcholine	Di-12:0-PC	21.0	−1 [88]
DMPC	1,2-Dimyristoyl-*sn*-glycero-3-phosphatidylcholine	Di-14:0-PC	25.4	24 [88]
DMPG	1,2-Dimyristoyl-*sn*-glycero-3-phosphatidylglycerol	Di-14:0-PG	23.9	23 [89]
DMoPC	1,2-Dimyristoleoyl-*sn*-glycero-3-phosphatidylcholine	Di-14:1c9-PC	19.2	<−20[c]
POPC	1-Palmitoyl-2-oleoyl-*sn*-glycero-3-phosphatidylcholine	16:0–18:1c9-PC	28.3	−2 [88]
POPE	1-Palmitoyl-2-oleoyl-*sn*-glycero-3-phosphatidylethanolamine	16:0–18:1c9-PE	28.3	25 [90]
POPG	1-Palmitoyl-2-oleoyl-*sn*-glycero-3-phosphatidylglycerol	16:0–18:1c9-PG	28.3	−2 [91]
DOPC	1,2-Dioleoyl-*sn*-glycero-3-phosphatidylcholine	Di-18:1c9-PC	26.8	−20 [88]
Lyso-OPC	1-Oleoyl-2-hydroxy-*sn*-glycero-3-phosphatidylglycerol	18:1c9-PC	n.a.[d]	n.a.[d]
CHOL	Cholesterol	–	n.a.[d]	n.a.[d]

[a] Hydrophobic thickness, according to [45].
[b] Gel to liquid crystalline phase transition temperature.
[c] Upper boundary, T_m not reported.
[d] Not applicable, as it does not form bilayers on its own.

of their relevant properties are listed in Table 2. The hydrophobic thickness of the bilayers was calculated from the following formulas [45]. For saturated acyl chains with n_c carbons the hydrophobic length L is given by $L(n_c{:}0) = 2.21(n_c - 2.5)$ Å, while for monounsaturated acyl chains $L(n_c{:}1) = 1.9(n_c - 3.9)$ Å. For POPC, POPG, and POPE, the average length for the two chains [palmitoyl (16:0) and oleoyl (18:1)] was used.

2.2. Peptide synthesis

The wild type MSI-103 and seven labeled analogues were synthesized as previously described using standard solid-phase peptide synthesis [22]. One selective Ala-d_3 label was incorporated in position Ala7, Ile9, Ala10, Gly11, Ile13, Ala14, or Ala17 (see Table 1). All labeled peptides retain their biological activity, as shown previously [22]. Macroscopically oriented NMR samples with full hydration were prepared as was described previously for MSI-103 in DMPC [22,41]. In short, peptides and lipids were co-solubilized in $CHCl_3$/MeOH, and the solution was spread on thin glass plates. The solvent was evaporated under vacuum, and the glass plates were stacked and hydrated at 96% relative humidity at 48 °C. In order to study the initial binding, or to address very low peptide concentrations, non-oriented multilamellar vesicle samples were prepared with deuterium-depleted water (Acros Organics, Geel, Belgium) at 1:1 lipid/H_2O (weight/weight) [41]. In these samples, the co-dissolved peptide–lipid mixture was dried to a film, and 50% (w/w) water was added. The homogenized samples were sealed in polyethylene bags. More details have been published previously [19].

2.3. Solid state NMR experiments

NMR experiments were carried out on 500 MHz and 600 MHz Bruker Avance NMR spectrometers (Bruker Biospin, Karlsruhe, Germany). ^{31}P-NMR was performed using a Hahn echo sequence with ^{1}H decoupling, and ^{2}H-NMR was performed with a solid echo sequence. Typical 90° pulse lengths were 4–5 μs. Further NMR experimental details have been published previously [22]. Oriented samples were usually measured with the bilayer normal parallel to the external magnetic field (0° tilt). Some ^{2}H-NMR samples (at least one for each lipid system) were also measured with the bilayer normal perpendicular to the magnetic field (90° tilt). Fast rotational diffusion of the peptides around the bilayer normal will lead to a scaling of splittings with a factor −1/2 in 90° tilt samples compared with 0° tilt samples, whereas in the absence of this rotation a powder-like line shape is observed at 90° tilt [46].

2.4. Calculation of peptide orientation and dynamics

For calculating the peptide orientation and dynamics, the structure of MSI-103 is assumed to be an ideal α-helix, based on a poly-alanine model generated with SYBYL (Tripos, St. Louis, USA) [24]. The orientation of the peptide in the macroscopically oriented membrane is described by the tilt angle (τ) and the azimuthal rotational angle (ρ), as illustrated in Fig. 1. Using ^{2}H-NMR data from all seven labeled positions, the helix orientation is calculated from rmsd fits and quadrupolar wave plots, as described in detail previously [19,22,23]. Peptide dynamics were accounted for using two different models, which are described in detail elsewhere [44]. In the "implicit" dynamical model, the local and global mobility of the peptide helix is simply described by an order parameter S_{mol}. This term reduces all ^{2}H quadrupolar splittings by a factor between 0 and 1, where 0 means complete isotropic averaging and 1 corresponds to no dynamics. In the "explicit" model, dynamics is described as Gaussian distribution of τ and ρ angles, with widths σ_τ and σ_ρ, respectively. Larger widths correspond to a more dynamic situation, with larger amplitudes of variation of the angles. It is assumed that the helix fluctuations are fast on the NMR time scale, so that the measured splittings are averages over the distributions [44].

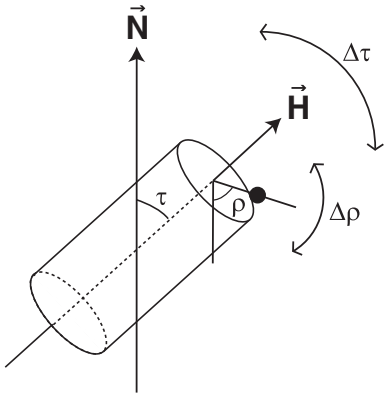

Fig. 1. The orientation of a helical peptide is described by the angles τ and ρ. The tilt τ is defined as the angle between the helix axis (***H***, directed from the N- to the C-terminus) and the bilayer normal (***N***). The azimuthal rotation angle ρ gives the orientation of side chains around the helix axis, and it is defined here as the angle between the radial vector through C^α of position 12 (the projection is marked with a black circle) and a reference orientation. Because of whole-body motions of the helix, the τ and ρ angles are not fixed but fluctuate within some range $\Delta\tau$ and $\Delta\rho$, respectively. In the present study, Gaussian distributions of τ and ρ are used to describe these dynamical modes.

We estimate the error of the orientation and dynamics parameters from the widths of the minima in the rmsd plots. For ρ the estimated accuracy is usually ±2°. For τ in the S-state the estimated accuracy is ±1°, and in the T-state it is ±3° in DMPC samples and up to ±12° in other systems. For σ_τ and σ_ρ the uncertainties are larger, but usually within ±10°.

3. Results

3.1. Acyl chain length and unsaturation

In our previous study on MSI-103, the peptide had been incorporated in DMPC (di-14:0-PC) [22]. All ^{2}H-NMR spectra and quadrupolar splittings from DMPC and DMPC/DMPG systems analyzed in the present work were taken from that previous study [22]. Our first comparative series now includes other PC lipids with longer chains (POPC (16:0–18:1-PC) and DOPC (di-18:1-PC)), with shorter chains (DLPC (di-12:0-PC) and DMoPC (di-14:1-PC)), and with different degrees of saturation. ^{2}H-NMR spectra of oriented samples at P/L = 1:50 are shown in Fig. 2. The orientation of the peptide in these membranes is calculated from the ^{2}H-NMR data as described in Materials and methods. The deuterium quadrupole splittings are analyzed using an explicit dynamical model as recently described in detail [44]. The experimental splittings are listed in Table 3, and the resulting best-fit orientations of the peptide are evaluated in terms of the helix tilt angle τ and the azimuthal rotation ρ (see Table 4). Error ranges are given in Appendix A (Table A1). The value of τ is defined as the angle between the helix axis and the membrane normal (see Fig. 1). Compared to our previous report, where an implicit dynamical model had been used for data analysis [22], some minor differences are seen here in the values of the orientational angles which are obtained using the explicit dynamical model. To demonstrate the validity of our results, i.e. that the conclusions are independent of either assumption, we also analyzed the data using the earlier implicit dynamical model in Appendix A (Table A2).

As a start, let us re-consider the original NMR data on MSI-103 in DMPC, as summarized in Tables 3 and 4. At very low peptide-to-lipid molar ratio (P/L) of 1:400 and below, MSI-103 assumes an S-state with a helix tilt angle of $\tau = 101°$ [22], just like PGLa [20]. This result had been obtained by ^{19}F-NMR, because ^{2}H-NMR is not sensitive enough for such low peptide concentrations in oriented samples. At

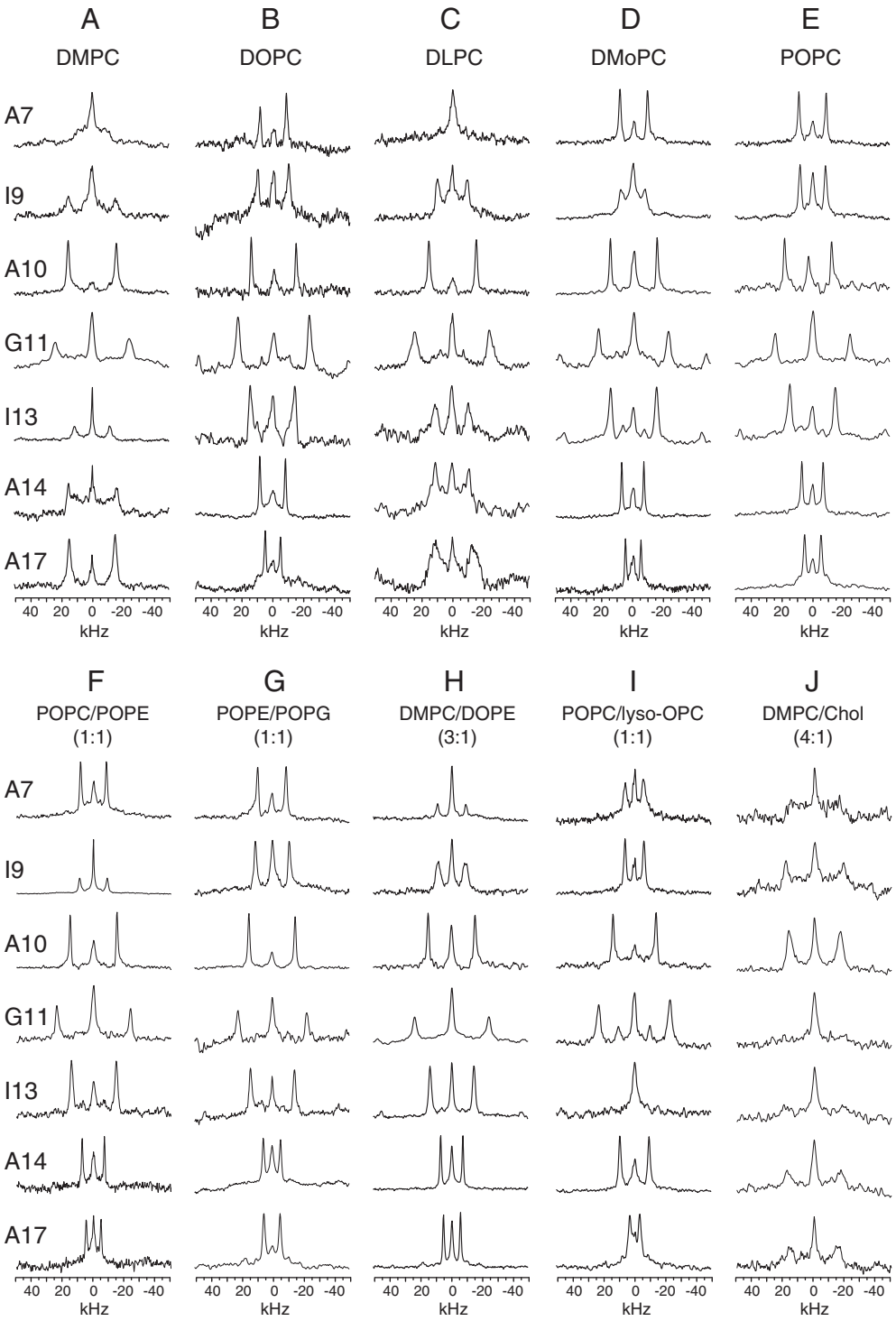

Fig. 2. ^{2}H-NMR spectra of Ala-d_3 labeled MSI-103 in oriented lipid bilayers, measured at a peptide-to-lipid ratio of 1:50. The labeled position is indicated on the left of each row of spectra. Representative systems shown here are: (A) DMPC; (B) DOPC; (C) DLPC; (D) DMoPC; (E) POPC; (F) POPC/POPE (1:1); (G) POPE/POPG (1:1); (H) DMPC/DOPE (3:1); (I) POPC/Lyso-OPC (1:1); (J) DMPC/CHOL (4:1). (The complete data with more lipids and for more P/L ratios is summarized in Table 3, giving also the experimental temperatures.)

an intermediate P/L of 1:200, our re-evaluation of the original ^{2}H-NMR data yields an angle of $\tau = 108°$. This value reflects a fast exchange between discrete S- and T-states, similar to the scenario reported for PGLa in DMPC at a lower threshold concentration [20]. Because the exchange is fast on the NMR time scale only one average orientation is obtained, as described by one set of distributions of τ and ρ. At high concentrations of P/L = 1:50 and above, our re-analysis of MSI-103 confirms the tilted T-state with $\tau = 127°$ [20,22].

In the present ^{2}H-NMR study MSI-103 was embedded in DOPC, with long unsaturated acyl chains, at the same concentrations as previously used for DMPC, namely P/L = 1:200, 1:50 and 1:20. ^{2}H-NMR spectra of ^{2}H-labeled MSI-103 in DMPC and DOPC at P/L = 1:50 are shown in Fig. 2A and B, respectively. The quadrupolar splittings from each labeled position (see Table 3) are analyzed by comparing the experimental data with the splittings calculated for different orientations of the peptide, as previously described [44]. The root mean

Table 3
Quadrupole splittings (in kHz) found for Ala-d_3 labeled MSI-103 in different lipid bilayers (*experimental values in italics*).

Lipid system	P/L	T (K)	Labeled position						
			Ala7	Ile9	Ala10	Gly11	Ile13	Ala14	Ala17
DMPC[a,b]	1:200	308	*8.6*	*12.0*	*24.0*	*48.2*	*4.0*	*14.8*	*13.4*
DMPC[b]	1:50	308	*17.0*	*30.4*	*31.2*	*47.5*	*22.8*	*31.0*	*29.7*
DMPC[b]	1:20	308	*2.0*	*28.5*	*35.2*	*~60*	*23.9*	*31.5*	*29.5*
DOPC[a]	1:200	303	*16.8*	*17.0*	*25.0*	*46.0*	*25.6*	*12.2*	*11.0*
DOPC	1:50	303	*17.0*	*20.1*	*29.1*	*46.3*	*29.3*	*16.6*	*9.9*
DOPC	1:20	303	*15.2*	*23.9*	*30.0*	*45.0*	*31.1*	*16.3*	*9.2*
DLPC[a]	1:200	303	*Iso*[c]	[d]	*Iso*[c]	[d]	*Iso*[c]	[d]	*Iso*[c]
DLPC	1:50	303	*7.0*	*19.3*[c]	*30.9*	*48.5*	*20.2*	*21.9*	*24.1*
DLPC	1:20	303	*2.0*	*26.9*	*30.8*	*48.0*	*21.1*	*21.3*	*26.0*
DMoPC	1:50	303	*17.8*	*16.0*	*30.3*	*45.3*	*29.8*	*14.3*	*10.0*
POPC	1:50	303	*17.7*	*16.4*	*30.5*	*48.5*	*29.5*	*13.8*	*10.6*
POPC/POPE (1:1)	1:50	303	*17.2*	*17.9*	*30.3*	*48.6*	*29.0*	*14.4*	*9.6*
POPE/POPG (3:1)	1:50	303	*16.9*	*20.9*	*29.8*	*39.0*	*29.9*	*12.9*	*11.1*
POPE/POPG (1:1)	1:50	303	*18.4*	*21.9*	*30.2*	*44.6*	*28.5*	*11.2*	*10.5*
DMPC/DOPE (3:1)	1:50	308	*18.2*	*17.7*	*30.2*	*48.1*	*28.7*	*14.4*	*11.0*
POPC/Lyso-OPC (2:1)	1:50	303	[d]	[d]	[d]	[d]	*31.4*	*17.5*	*8.2*
POPC/Lyso-OPC (1:1)	1:50	303	*11.9*	*12.2*	*27.9*	*46.2*	*4.0*	*18.9*	*6.4*
DMPC/CHOL (4:1)	1:50	303	*31.0*	*37.4*	*33.0*	*36.0*	*37.3*	*35.0*	*34.0*

[a] MLV samples: splittings doubled for comparison.
[b] From [22].
[c] Isotropic component too dominant to measure splitting in MLV sample.
[d] Not measured.

square deviation (rmsd) is a measure of the quality of the fit to the four parameters τ, ρ, σ_τ, and σ_ρ. Since we estimate the error in the quadrupolar splittings to be around 1 kHz, rmsd values below 1 kHz should be considered a perfect fit. However, we assume a perfect α-helical structure and use a simplified dynamic model, so in view of these approximations somewhat larger best-fit rmsd values might be obtained. The quality of the fit is assessed by helical wave plots and rmsd analysis. (In Appendix B helical wave and rmsd plots are given for all studied systems.)

Fig. 3A shows the best-fit quadrupolar wave through the experimental splittings for MSI-103 in DOPC at 1:50. To check whether any alternative solutions with similar rmsd are present (i.e. any other local minima), the rmsd is plotted in Fig. 3B for all combinations of the peptide tilt and azimuthal angles. The color code indicates the lowest rmsd value for each pair of τ and ρ angles that can be obtained with any values of σ_ρ and σ_τ. The inset shows a complementary plot of the lowest rmsd values for each pair of σ_ρ and σ_τ values, with any values of τ and ρ. These two plots are different projections of the four-dimensional parameter space, and points in the two plots with the same color correspond to the same parameter values. For example, all the black points in the σ_ρ–σ_τ plot correspond to the black points in the τ–ρ plot, representing the parameter values for which rmsd is below 3.4 kHz. It is clear from Fig. 3A/B that the helix orientation of MSI-103 in DOPC at 1:50 is very well defined, there is one clear minimum at $\tau = 94°$, and $\rho = 133°$, and it is compatible with a somewhat wider range of dynamics (i.e., several combinations of σ_ρ and σ_τ give similar rmsd values). Also at a low peptide concentration of 1:200 as well as at the highest P/L = 1:20 the same S-state is found (see Table 4), with only minor changes of the best-fit parameters within the error of the method. In other words, the MSI-103 peptide does not show a concentration-dependent reorientation from S- to T-states in DOPC bilayers, unlike the situation in DMPC. Given that this difference is detectable at P/L ratios of 1:50 and 1:20, these concentrations will be examined in the following lipid systems.

The MSI-103 spectra in short-chain saturated DLPC (see Fig. 2C) showed well defined splittings (see Table 3), and gave a tilted T-state for P/L = 1:50 (see Fig. 3C/D, Table 4) with $\tau = 123°$, $\rho = 105°$, and $\tau = 123°$, $\rho = 107°$ for 1:20, just like in DMPC. On the other hand, in DMoPC (di-14:1-PC, for spectra see Fig. 2D), which has short unsaturated acyl chains, the peptide maintains an S-state at 1:50 with $\tau = 95°$, $\rho = 133°$, just as in DOPC. POPC (16:0–18:1-PC, for spectra see Fig. 2E), with one saturated and one unsaturated acyl chain, has a larger hydrophobic thickness than DOPC, and in this lipid system the best fit values of $\tau = 96°$, $\rho = 132°$ are again very similar to the S-state in DOPC.

We note at this point some limitations on the use of macroscopically oriented samples, which turn out be instructive for the discussion below. All samples with P/L = 1:50 and 1:20 were prepared in oriented bilayers, as usual for the ^{2}H-NMR orientational analysis. Samples with a low peptide concentration of 1:200, however, had to be measured as non-oriented multilamellar vesicles (MLVs). This was necessary to accommodate a sufficient amount of labeled peptide in the NMR probe, given the intrinsically low sensitivity of ^{2}H-NMR. The resulting MLV powder spectra (see Fig. 4) provide essentially the same information as the oriented samples, but all splittings are averaged by a factor of 1/2 due to fast rotation of the peptide around the bilayer normal [41]. Therefore, the Pake splittings from the MLV samples are multiplied by a factor of 2 in Table 3 for the analysis in Table 4. It is important to realize, however, that MLVs are hydrated 1:1 with H_2O (weight/weight) and therefore contain some excess water, whereas oriented membranes prepared at 96% relative humidity contain no such excess. The extra water in MLVs allows the peptide to exchange between the membrane-bound state and the free form in bulk solution, unless the peptides are electrostatically attracted or strongly bound to the lipids. This has been shown by ^{19}F-NMR on PGLa in solution with DMPC/DMPG vesicles [47]. In contrast, oriented samples contain no excess H_2O, so that no bulk water phase is present, hence the peptides are always in contact with the membrane [20]. The powder spectra shown in Fig. 4 therefore allow us to assess the binding affinity of MSI-103 to MLVs composed of different lipids. In DMPC (Fig. 4A), the spectra of all labels (A7, A10, A17 shown here) are dominated by an isotropic signal, which represents free peptide in the bulk water phase. (Traces of HDO in the

Table 4
Best-fit orientation and dynamics parameters for MSI-103 in different lipid bilayers (*obtained results in italics*).

Lipid system	P/L	τ (°)	ρ (°)	σ_τ (°)	σ_ρ (°)	Rmsd (kHz)	Rapid diffusion	State
DMPC[a]	1:400	*101*[a]	*130*[a]			*1.1*	*Y*[a]	*S*[a]
DMPC[b]	1:200	*108*	*120*	*6*	*24*	*1.2*	*Y*	*S↔T*
DMPC[b]	1:50	*127*	*100*	*3*	*2*	*3.4*	*N*	*T*
DMPC[b]	1:20	*126*	*109*	*0*	*0*	*3.8*	*N*	*T*
DOPC	1:200	*95*	*134*	*0*	*19*	*2.8*	*Y*	*S*
DOPC	1:50	*94*	*133*	*0*	*14*	*3.2*	*Y*	*S*
DOPC	1:20	*93*	*134*	*0*	*13*	*2.8*	*Y/N*	*S*
DLPC[c]	1:200	*n.a.*[c]	*n.a.*[c]	*n.a.*[c]	*n.a.*[c]	*n.a.*[c]	*n.a.*[c]	*n.a.*[c]
DLPC	1:50	*123*	*105*	*0*	*18*	*1.4*	*N*	*T*
DLPC	1:20	*123*	*107*	*0*	*22*	*1.3*	*N*	*T*
DMoPC	1:50	*95*	*133*	*0*	*15*	*3.8*	*Y*	*S*
POPC	1:50	*96*	*132*	*0*	*13*	*3.5*	*N*	*S*
POPC/POPE (1:1)	1:50	*95*	*133*	*0*	*14*	*3.4*	*Y*	*S*
POPE/POPG (3:1)	1:50	*93*	*135*	*0*	*18*	*3.3*	*Y*	*S*
POPE/POPG (1:1)	1:50	*94*	*135*	*0*	*16*	*3.2*	*Y*	*S*
DMPC/DOPE (3:1)	1:50	*96*	*133*	*0*	*14*	*3.3*	*Y*	*S*
POPC/Lyso-OPC (2:1)[c]	1:50	*93*[d]	*134*[d]	*n.a.*	*n.a.*	*n.a.*	*N*[d]	*S*[d]
POPC/Lyso-OPC (1:1)	1:50	*112*	*113*	*19*	*14*	*4.1*	*N*	*S↔T*
DMPC/CHOL (4:1)[e]	1:50	*n.a.*[e]	*n.a.*[e]	*n.a.*[e]	*n.a.*[e]	*n.a.*[e]	*N*	*aggr.*

[a] ^{19}F-NMR analysis from [22] based on the implicit dynamical model.
[b] ^{2}H-NMR data from [22], re-analyzed using the explicit dynamical model.
[c] Dominant isotropic signal from free peptide in MLV sample did not allow data analysis.
[d] Inferred from the fact that splittings are similar to those for MSI-103/DOPC 1:20.
[e] Static powder signal of aggregated peptide in oriented sample did not allow data analysis.

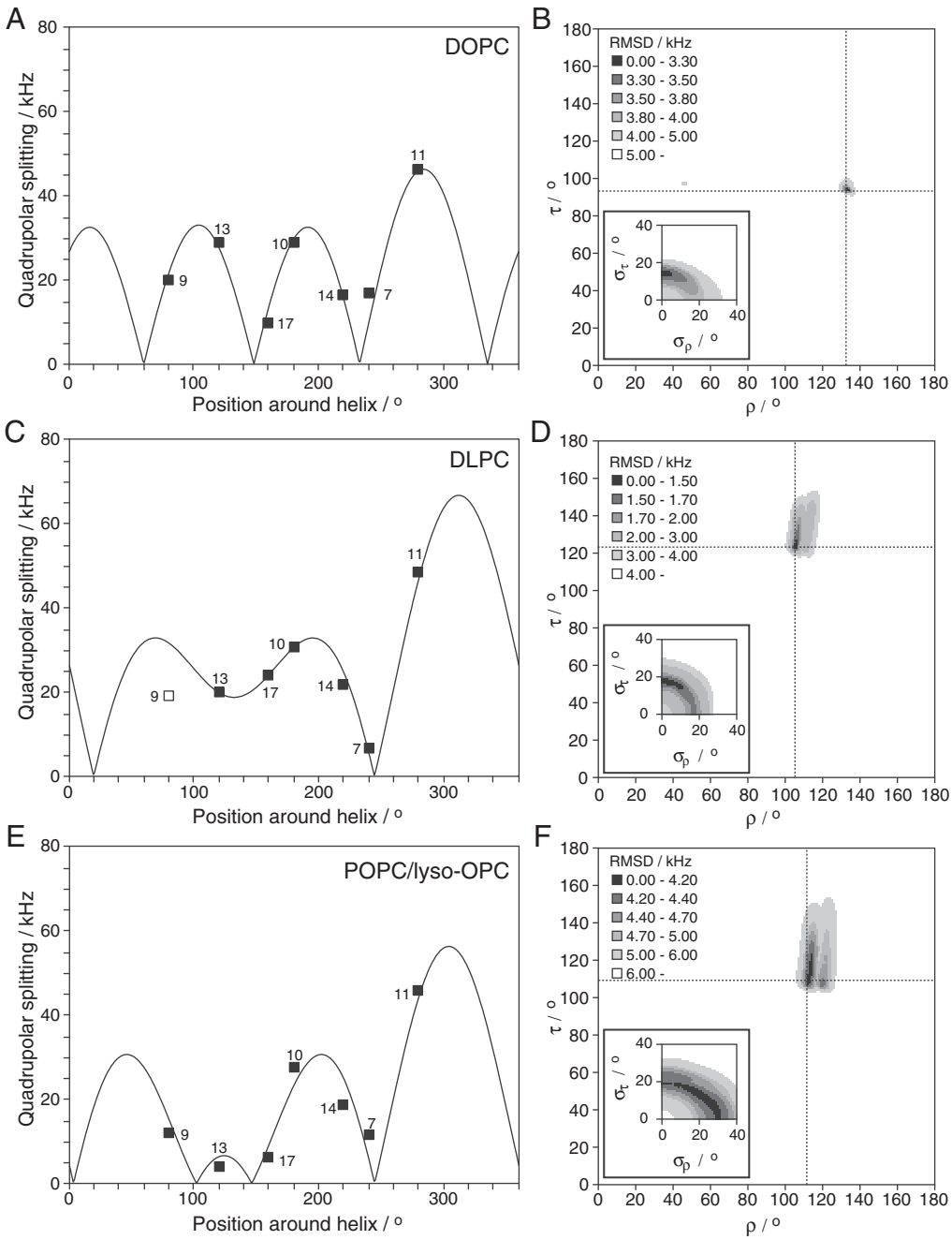

Fig. 3. Best-fit quadrupolar waves (A, C, E) and rmsd plots (B, D, F) calculated from the ^{2}H-NMR data of MSI-103 in selected lipid systems at P/L = 1:50. (A/B) DOPC; (C/D) DLPC; (E/F) POPC/lyso-OPC (1:1). Experimental quadrupolar splittings for different labeled positions are marked with filled squares. *Footnote*: In DLPC the splitting from position Ile9 did not fit with the other data, and was not used in this fit (unfilled square). When it was included, a similar helix orientation was found but with a higher rmsd of 3.4 kHz (compared to 1.3 kHz). Corresponding color plots for all of the studied peptide–lipid systems are compiled in Appendix B.

deuterium-depleted water are considered to be marginal in this qualitative comparison). In contrast, the intensity of this spectral component is much weaker in DOPC (Fig. 4B), suggesting that DOPC binds the peptides much tighter than DMPC. In this respect, DOPC is very similar to anionic DMPC/DMPG (Fig. 4C), for which it is known that cationic MSI-103 is attracted by electrostatic interactions [22]. A comparison with the short-chain saturated lipid DLPC (di-12:0-PC) in Fig. 4D finally shows that at P/L = 1:200, the MLV spectra were very poor. For most labeled peptides only a huge isotropic peak was observed and no resolved splittings were found. It thus seems that MSI-103 does not bind well to DLPC at all, and no orientation could be determined in the presence of excess water.

3.2. Lipid head groups

The above studies on MSI-103 were done in uncharged PC lipids, which are common in eukaryotic membranes [38] and have been used in most NMR studies of AMPs [5]. To investigate the influence of lipid head groups, MSI-103 was next embedded in different types of lipids but with the same acyl chains. All samples were prepared with P/L = 1:50, because here the interesting re-alignment from S- to T-states is most suitably detected. The effect of negatively charged lipids had been previously investigated, and no difference was found in oriented samples of DMPC/DMPG (3:1) compared to DMPC for either MSI-103 [22] or PGLa [20]. An effect of lipid charge is seen only in MLV

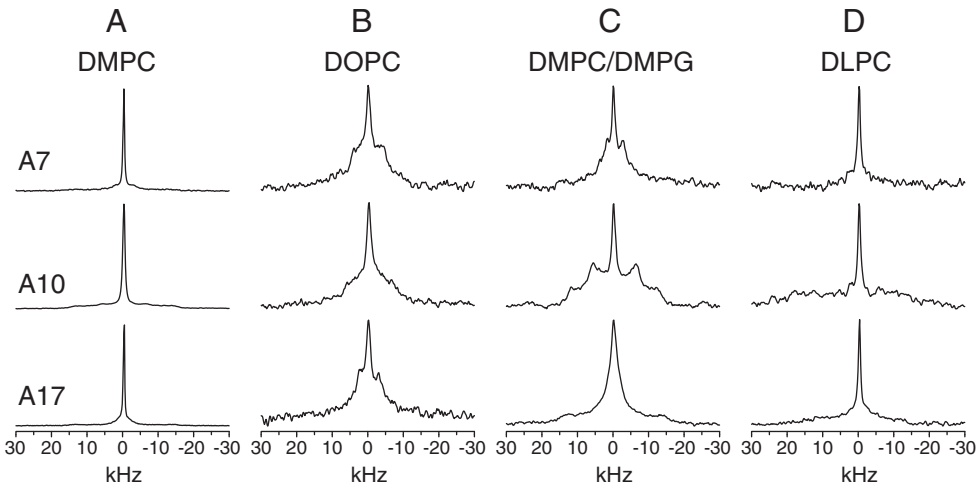

Fig. 4. Representative ^{2}H-NMR spectra of Ala-d_3 labeled MSI-103 (positions Ala7, Ala10, Ala17) in different lipid systems at a low peptide concentration (P/L = 1:200). These samples were prepared as multilamellar vesicles containing excess water (1:1 weight/weight). (A) DMPC; (B) DOPC; (C) DMPC/DMPG (3:1); (D) DLPC. All spectra are scaled to the isotropic intensity arising from unbound peptide, hence the proportions of bound and unbound peptide correspond roughly to the proportions of area of the powder component and the area of the isotropic central peak.

samples containing excess water (Fig. 4A/C), due to the electrostatic affinity of the cationic peptides to anionic bilayers.

In the present study we focus on the effect of lipid head groups with different intrinsic curvature. PE lipids have a smaller head group than PC and are very common in bacterial membranes. POPE has a tendency to form an inverted hexagonal H_{II} phase, given its pronounced negative curvature. In our experiments it was mixed with POPC or POPG to maintain stable lamellar bilayers. On the other hand, lyso-PC carries only a single acyl chain; hence the resulting positive curvature favors the formation of micelles. Lyso-OPC was therefore mixed with POPC to form stable lamellar membranes. Lipids with one palmitoyl and one oleoyl chain were used here, since many natural phospholipids carry this combination [48], and they are the most common acyl chains in *Escherichia coli* lipids [49,50]. All of these lipids are in the liquid crystalline phase at 30 °C, the temperature where the ^{2}H-NMR measurements were performed.

To allow comparison with pure POPC, we examined MSI-103 in POPC/POPE (1:1) (spectra are shown in Fig. 2F) and found the same S-state ($\tau = 95°$ and $\rho = 133°$). The peptide was also investigated in anionic POPE/POPG (3:1), which corresponds closely to the *E. coli* inner membrane composition [51], as well as in POPE/POPG (1:1); ^{2}H-NMR spectra for POPE/POPG (1:1), are shown in Fig. 2G. The helix orientation in these two systems with $\tau = 93°$ and $\rho = 135°$ was found to be almost identical to the S-state in pure POPC (see Tables 3 and 4). Therefore, no effect of lipid head groups was detected in these unsaturated PO-bilayers with negative curvature, irrespective of lipid charge. Even in DMPC/DOPE (3:1) (for spectra see Fig. 2H) the S-state was found ($\tau = 96°$ and $\rho = 133°$), in contrast to pure DMPC which favors the T-state at P/L = 1:50 (see Fig. 2A, and Tables 3 and 4).

Next, lipid mixtures with a positive curvature were analyzed. In POPC/lyso-OPC (2:1), several representative labels on MSI-103 gave essentially the same splittings as in POPC (see Table 3), supporting the S-state. However, in the presence of more lyso-OPC, at a POPC/lyso-OPC ratio of 1:1, these splittings changed compared to those measured in POPC; hence the full series of seven Ala-d_3 labels was prepared and measured. Spectra are shown in Fig. 2I, and the data analysis gives a state with an intermediate tilt of $\tau = 112°$, $\rho = 113°$, and a rather high rmsd of 4.1 kHz. This is similar to the behavior of MSI-103 in DMPC at low concentration (P/L = 1:200) and suggests a fast exchange between S- and T-states, as previously described for PGLa [20]. The rmsd plot and best-fit curve are illustrated in Fig. 3E/F. Compared to the situation in DOPC and DLPC at P/L = 1:50, the helix orientation (τ, ρ) is less well-defined in POPC/lyso-OPC (1:1), and a rather wide range of dynamics parameters (σ_τ, σ_ρ) give similar rmsd values. It is nevertheless clear that the best fit has a high value of σ_τ, indicating a large variation in the tilt angle, as expected for a peptide in fast exchange between two states with different tilt angles, like the S- and T-states.

Finally, MSI-103 was examined in DMPC/cholesterol (4:1) bilayers, chosen to resemble eukaryotic plasma membranes [38]. In this case, all oriented samples gave powder line shapes with the maximum possible Pake splitting of ~35 kHz, which is typical for static peptides that are immobilized in extended aggregates (see Fig. 2J). These peptides are no longer oriented with respect to the membrane; hence tilt angles cannot be meaningfully described.

3.3. Peptide dynamics

In the present ^{2}H-NMR data analysis we used an explicit dynamic model, as previously described in detail [44]. This model accounts for the whole-body fluctuations of the rod-like peptide helix. It allows for a Gaussian distribution over the τ and ρ angles, assuming that a fast exchange between these different orientations gives an averaged splitting. This dynamical information is presented as the respective widths, σ_ρ and σ_τ, of the two mobility distributions. Large values of σ_ρ and σ_τ correspond to highly mobile peptides, whereas e.g. $\sigma_\tau = 0°$ would implicate that the preferred tilt angle of the helix long axis does not fluctuate significantly.

In unsaturated lipids, the dynamic behavior of MSI-103 is very similar in all cases. The peptide assumes an S-state with $\sigma_\rho = 15°$, indicating a certain degree of wobble around the helix long axis. On the other hand, σ_τ is always found to be 0°, corresponding to a perfectly well-defined τ angle. In saturated lipids, on the other hand, several different types of motion are observed. At high concentration in DMPC, i.e. in the T-state, the peptides are virtually immobile. A more mobile situation is found in DMPC at P/L = 1:200 (with $\sigma_\tau = 6°$ and $\sigma_\rho = 24°$), and in POPC/lyso-OPC (1:1) at P/L = 1:50 (with $\sigma_\tau = 19°$ and $\sigma_\rho = 14°$). The actual best-fit values given here (see Table 4) need not reflect the true situation precisely, since Fig. 3E/F shows that a range of σ_ρ and σ_τ combinations correspond to similar rmsd values. This ambiguity might be due to insufficient data and could improve if more data were available. Nevertheless, both in DMPC at P/L = 1:200 and in POPC/lyso-OPC, the fits suggest a more dynamic situation for MSI-103, in agreement with our interpretation above that the peptide is engaged in fast exchange between the S- and T-states in these cases.

In order to allow a comparison with previous studies, we also performed the fits using the more traditional implicit dynamic model. In that simple model, dynamics is included only in the form of an order parameter S_{mol}, which can take a value between 0 and 1 and has the effect of averaging all splittings by this constant factor. The implicit dynamics method has been used extensively, for example in studies of PGLa and MSI-103 [19–23]. The results on our present MSI-103 systems are listed in Appendix A, Table A2. Briefly, the obtained best-fit orientations (in terms of τ and ρ) do not change much when this method is used. In most cases, the rmsd of the fit is lower when the explicit model is used, as can be expected from the increased number of fitting parameters. The largest improvement of rmsd is found for the most mobile cases, showing that the explicit model gives a better representation of whole-body dynamics, while for the less mobile cases the choice of dynamic model has only a small influence on the fit.

A rather different type of mobility concerns the fast rotational diffusion of peptides in the bilayer plane, which effectively shows up as a long-axial rotation of the molecule around the membrane normal. This kind of motional averaging does not influence the NMR spectra of samples that are oriented with the bilayer normal along the static magnetic field direction. However, when the sample is tilted by 90° relative to the magnetic field, this fast rotational diffusion will average splittings with a factor −1/2, whereas in the absence of this rotation a powder-like line shape is observed. The occurrence of rotational diffusion of MSI-103 in the bilayer was thus examined in different lipid systems by manually tilting the oriented sample, and our findings are summarized in Table 4. Some representative ^{2}H-NMR spectra at 0° and 90° tilt are shown in Appendix C. In most cases rotational diffusion is fast in the S-state (on the ^{2}H-NMR millisecond time scale), but it is absent in the T-state. This behavior suggests that the T-state may correspond to some oligomeric or more deeply inserted state where diffusion is slowed down. An exception is seen in POPC (P/L = 1:50), where the peptides are in the S-state but do not diffuse rapidly. Similarly, in DOPC at P/L = 1:20, some of the labeled samples showed fast averaging and others not. The helixes nevertheless remain well oriented throughout, suggesting that a very high surface coverage the peptides may simply block each other from diffusing freely in the membrane.

4. Discussion

Using solid-state ^{2}H-NMR on selectively Ala-d_3 labeled MSI-103, we have determined the orientation of this amphiphilic α-helical peptide in membranes of different lipid compositions and at different peptide concentrations. This regular sequence has a high antimicrobial activity and serves as a good representative of many other antimicrobial peptides, e.g. PGLa from the magainin family. First, we will discuss the preferred alignment states and re-alignment behavior of MSI-103 in the different lipid systems. Then we will compare our results with previous studies of the orientation of membrane-active peptides in different lipid systems. Finally, the results will be interpreted in terms of lipid geometry and spontaneous membrane curvature.

4.1. MSI-103 in different lipid systems

In the present analysis, the helix tilt (τ) and azimuthal rotation angle (ρ) of MSI-103 have been determined in a wide range of lipid systems. The ^{2}H-NMR strategy is highly sensitive to variations in helix orientation, giving more accurate angles (and validating the unperturbed helical conformation at the same time) than most other methods. The last column in Table 4 summarizes our results in terms of the observed orientational states of MSI-103 in different lipid system, i.e. the surface-bound S-state and the tilted T-state. For various PC lipids, we analyzed several different peptide-to-lipid ratios, i.e. P/L of 1:200, 1:50 and 1:20, because the re-alignment from the S-state to the T-state is expected to occur somewhere in this range. The threshold concentration P/L* for re-alignment obviously depends on the type of lipid system employed and on the specific experimental conditions (temperature, hydration, etc.), just as the P/L* values differ from one peptide to another. Of course it would be most informative to present the actual threshold value P/L* for MSI-103 for each different lipid system. This would require examining its behavior over many P/L ratios and constructing a proper phase diagram. However, in view of the enormous experimental effort of having to prepare 7 different NMR samples for each data point in this phase diagram, such detailed analysis was not feasible. Instead, we focused on the P/L ratio of 1:50, given that the alignment state of MSI-103 observed at this intermediate concentration clearly shows its fundamental propensity to favorably re-align in a particular lipid system or not. Under these conditions we were thus able to compare the peptide alignment for many different types of lipids, by systematically varying the lipid acyl chain length, the degree of unsaturation, the lipid head group type, and – last but not least – purposefully the spontaneous curvature of the lipid bilayer.

It can be noted that in unsaturated lipids, the rmsd of the best fit is always quite large, 3–4 kHz, while in saturated lipids, better fits are found, down to 1.4 kHz. As discussed in Appendix A, this might be due to small deviations of the structure from an ideal α-helix in unsaturated lipids, and when one data point is left out much better fits are found, with rmsd of 0.9–2.1 kHz, but with almost no change in orientation or dynamics (see Table A3 in Appendix A). Thus, our discussion here is not influenced by these possible structural effects.

From a previous analysis of MSI-103 in the saturated lipid DMPC, we know that it assumes the S-state at low peptide concentration (P/L ≤ 1:400). At higher concentrations, beyond a threshold of about P/L* = 1:200, the helix re-aligns into the T-state [22]. The S-state is commonly assumed to represent monomeric peptides, while the distinctly different T-state might be attributed to peptide dimerization [22,23]. This T-state is observed here also in DLPC, another saturated phospholipid with short chains. On the other hand, in all PC lipid systems with unsaturated acyl chains we always found the S-state, irrespective of peptide concentration or lipid head group type. Only when lyso-lipids are added does the T-state become accessible for MSI-103 in bilayers with unsaturated acyl chains. Fig. 5 gives an overview of the helix tilt angle as a function of acyl chain length in PC lipids. It is clear that there is no correlation between tilt and chain length. On the other hand, there is a remarkable similarity of the respective tilt angles in all saturated lipids on the one side, and all unsaturated lipids on the other side. We thus conclude that the hydrophobic thickness per se is not a determining factor for peptide orientation in these cases, but unsaturation is a key parameter.

In the presence of unsaturated acyl chains, no change in tilt angle is observed for various different head group compositions. MSI-103 always assumes the S-state in POPC, POPC/POPE, and POPE/POPG. This observation suggests that even if there was an effect of lipid head group (such as size and charge), this influence is smaller than the effect of unsaturation. Even when only 25 mol% DOPE was added to DMPC, the S-state was induced, rather than the T-state that is preferred in pure DMPC. On the other hand, when 20 mol% cholesterol was added to DMPC, all ^{2}H-NMR spectra show powder line shapes with a maximum splitting. In these cases the peptides are no longer oriented in the bilayer, and are most likely excluded from the membrane to form large immobilized aggregates.

Bacterial membranes usually contain a high proportion of anionic lipids like PG, and they are also rich in PE. The mixture POPE/POPG (3:1) thus corresponds closely to the *E. coli* inner membrane [51]. Eukaryotic plasma membranes contain mainly PC and cholesterol, with only minor amounts of charged lipids, which are also mostly localized in the inner leaflet of the membrane, so that the cell surface is essentially uncharged [52]. It is generally accepted that the cationic peptides have a high affinity for the anionic bacterial membranes, which can partly explain the selectivity of these antimicrobial agents. Our results in multilamellar vesicle samples, which contain an

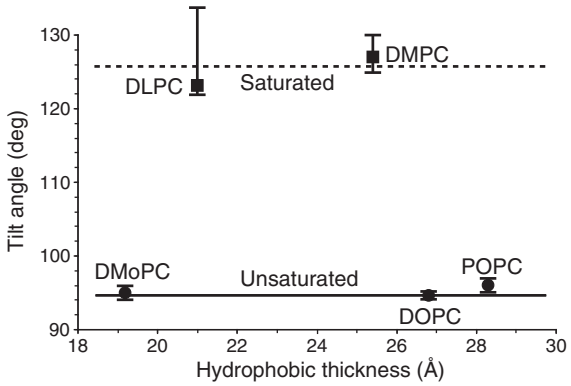

Fig. 5. Tilt angle of MSI-103 at P/L = 1:50 in PC lipids with different acyl chains, namely DMPC, DLPC, DMoPC, POPC and DOPC (as indicated). The observed tilt angles from Table 4 are plotted against the hydrophobic thickness of the respective lipid bilayer listed in Table 2. Squares represent saturated chains and circles unsaturated chains. Error bars show the ranges according to Table A1 in Appendix A.

excess of bulk water, confirm this electrostatic effect (see Fig. 4). However, once the peptides are trapped near the membrane surface (as in our oriented samples at 96% humidity), it seems that the alignment preference of MSI-103 is not affected by lipid charge. The same S-state was previously observed in DMPC and in DMPC/DMPG for both MSI-103 [22] and PGLa [20], and the same S-state is seen here in POPC, in POPC/POPE (1:1) and in POPE/POPG (1:1 and 3:1). Cholesterol, on the other hand, has a well known "sealing" effect and probably excludes the peptide from the membrane. This can explain the relative degree of protection of eukaryotic cells from the action of antimicrobial peptides. Our results in model membranes therefore support the notion that both electrostatics (affects peptide attraction) and cholesterol content (affects peptide binding) are important factors in explaining the selective activity of cationic antimicrobial peptides.

4.2. Lipid shape/spontaneous curvature model

The morphology of lipid assemblies (such as lamellar bilayers, micelles, hexagonal phases) can be described in terms of the shape of the lipid molecules. They can roughly be classified as cones with a small head group and larger acyl chain cross-sectional area, as cylinders with similar areas of head groups and acyl chains, or as inverted cones [53,54]. In Fig. 6A we illustrate this concept of relative size of head groups and acyl chains, which has important implications even for lamellar bilayers. The lipids used in this study are ranked here as a function of their relative shapes, according to their respective head groups and acyl chains (Lyso-OPC > DLPC > DMPC > DMoPC > POPC > DOPC > POPE > DOPE). For lipids with a small head group like PE, there is some "void space" in the head group region of a flat membrane, while PC lipids with larger head group have a more tightly packing head group region and a relatively higher degree of "void space" in the acyl chain region. In the lamellar phase the lipids are on average cylinder-shaped, meaning there is some stress on lipids which have another preferred shape. The "void space" should be seen as the empty space that would be present if the lipids would pack with their preferred shape. The amount of "void space" can be estimated from the spontaneous curvature of the lipid, which can be measured experimentally. Lipids such as PE have a large negative curvature and spontaneously form inverted hexagonal phases. On the other hand, lipids with a relatively large head group, like lyso-PC with only one acyl chain, has a large positive curvature and can form micelles.

Values of spontaneous curvatures have been reported in the literature, but they are not available for all lipids, and especially for PC lipids there is not much data available. Here, we will refer to the radius of spontaneous curvature (R_0). It should be noted that small values of R_0 correspond to high curvature, while a relaxed flat bilayer would have infinite R_0. PE lipids clearly have a pronounced negative spontaneous curvature, with several studies determining R_0 to be around −30 Å for DOPE [55–59]. It is also obvious that lyso-PC lipids have a large positive spontaneous curvature, with an R_0 value around +38 Å for lyso-OPC [60]. By comparison, lyso-OPE lipids with small head groups and a single acyl chain have a small curvature with R_0 larger than 400 Å and unclear sign, meaning they form essentially flat bilayers [55,60]. PC lipids, with a large head group and two acyl chains, have relatively small spontaneous curvatures. DOPC has a negative curvature, with an R_0 value of about −140 Å [61,62]. For POPC, no definite value is known, but there are indications that it also has a slight negative curvature [63]. DOPG also has a negative curvature, but this is strongly dependent on the ions present [64]. We may assume that POPG, too, has a similar spontaneous curvature. Thus, for all of the systems with unsaturated lipids used in this study, the lipids have a negative spontaneous curvature, except for the POPC/lyso-OPC mixture, where it is positive. We can thus conclude that there is a strong correlation between spontaneous curvature and the tilted state of MSI-103. The surface-bound S-state has tilt angles close to 90° (and appropriately oriented azimuthal angles) for all cases of negative spontaneous curvature.

It would be particularly interesting for the present study to compare the spontaneous curvatures of the different saturated and unsaturated PC lipids used. Unfortunately, to our knowledge no experimental data is available, except for DOPC. Nevertheless, it is known that PC lipids with short saturated acyl chains, like DHPC (di-6:0-PC), form micelles, and must therefore have a large positive spontaneous curvature. Longer-chain PCs do not form micelles, so they must have a lower positive curvature. According to one estimate, R_0 is in the range +33 Å to +50 Å for DMPC [62]. This might be an unrealistically strong curvature for DMPC, but we can surely take it to be positive, and we may also assume a somewhat larger, positive R_0 value for DLPC. When DMPC is mixed with DOPE, an overall negative curvature can be expected. No data is available for the spontaneous curvature of DMoPC, but the unsaturated chains must make it negative as well. Altogether, when considering the simple lipid shape concept illustrated in Fig. 6, we can conclude that there is a distinct correlation between the spontaneous curvature of the lipid system and the ability of MSI-103 to attain the T-state orientation. In systems with a negative spontaneous curvature only the S-state is observed, while in systems with positive spontaneous curvature a tilted state is accessible at sufficiently high peptide concentration.

Another way of describing a lipid system is by so-called lateral pressure profiles [65,66]. The main idea is that the lateral pressure of the membrane is not constant across the bilayer, but can be higher or lower at different cross-sections along the membrane normal. Roughly speaking, a negative spontaneous curvature corresponds to a higher lateral pressure in the acyl chain region than in the head group region, while a positive spontaneous curvature corresponds to a higher pressure in the head group region than in the acyl chain region. Using this picture, we can illustrate the binding of peptides to these different types of membranes. The model is illustrated in Fig. 6B/C. With negative spontaneous curvature, there is "void space" or low pressure in the head group region, so the peptide can easily bind and be accommodated in the head group region. However, it is hard for the peptide to insert deeper, because of the high lateral pressure in the acyl chain region. On the other hand, with positive spontaneous curvature, it will be harder for the peptide to bind to the membrane surface, because of the higher lateral pressure in the head group region. However, once the peptide is bound, it will be easier to insert more deeply into the membrane, displacing both the head groups and the acyl chains of the lipids.

These predictions can be qualitatively supported by the differential binding affinities of MSI-103 to MLVs in excess water. Fig. 4 shows

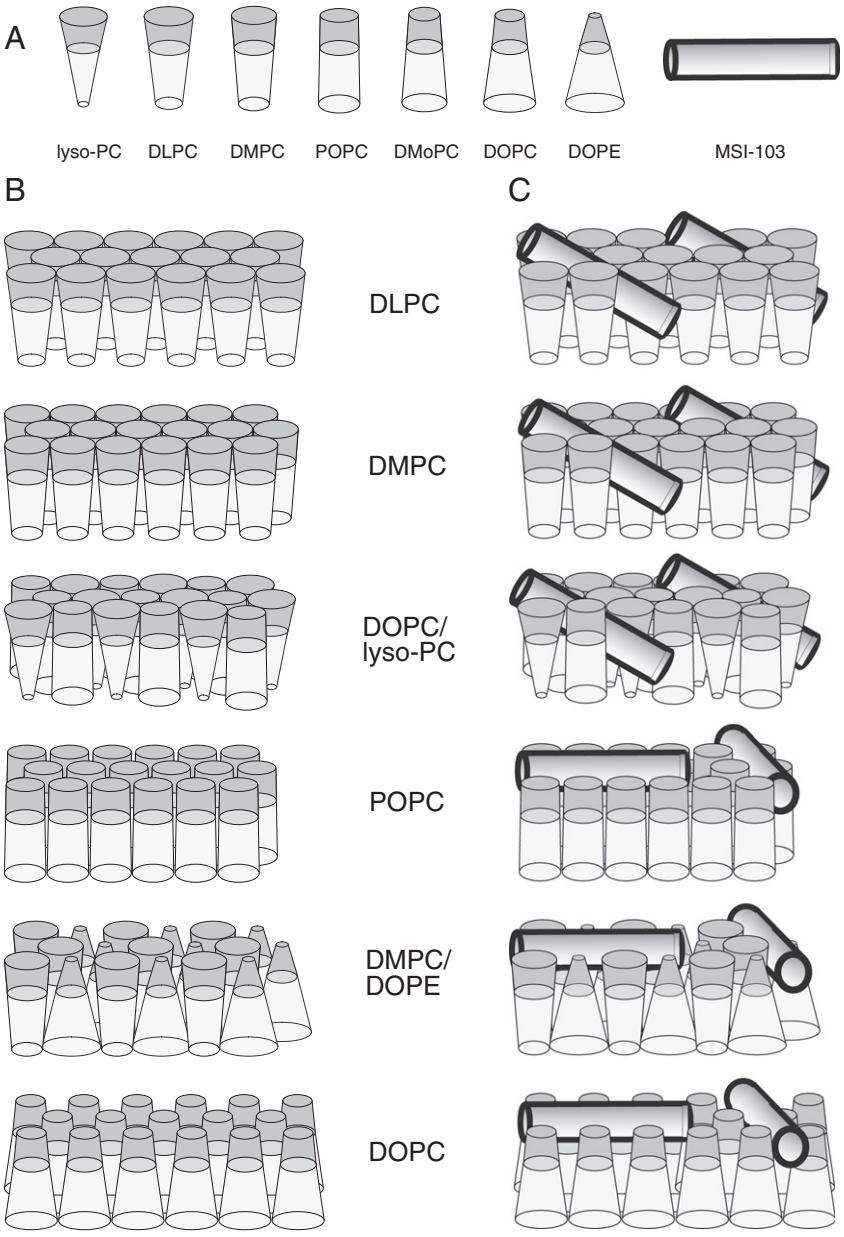

Fig. 6. Cartoon of lipid shapes. (A) Shapes of the different lipids used here, in order of decreasing spontaneous curvature. (B) Illustration of flat monolayers formed by the corresponding lipids, indicating the spontaneous shape as empty space to imply frustration. (C) Monolayers with added peptide, showing the helix orientation according to our ^{2}H-NMR results at P/L = 1:50 (see Table 4). MSI-103 assumes a tilted T-state in lipid bilayers with positive curvature, while it remains in the surface-bound S-state in systems with negative curvature.

that the free peptide binds much better to DOPC bilayers (negative spontaneous curvature) than to DMPC (small positive spontaneous curvature), and very poorly to DLPC (larger positive spontaneous curvature). The ability of DOPC to favorably accommodate the amphiphilic MSI-103 in the head group region thus affects the binding equilibrium in a comparable way as does the electrostatic effect of including anionic DMPG in the DMPC vesicles. Previously, it was found that the amphipathic α-helical peptide A18 has an increased affinity for membranes composed of POPC/DOPE and POPC/monoolein compared to POPC membrane, and the affinity increases with the amount of non-lamellar lipid, i.e. with larger positive curvature [67,68].

4.3. Comparison with other studies

The orientational behavior of MSI-103 can be expected to be very similar to that of PGLa, since they have similar sequences. The same kind of orientational states have indeed been demonstrated in DMPC, though with different threshold concentrations P/L* [19,20,22,23,33]. Using ^{15}N-NMR, it was recently shown that PGLa is in an S-state in di-20:1-PC and POPC, slightly inserted (T-state) in DMPC/DMPG (3:1) and di-10:0-PC, and even more inserted in DLPC [69]. All systems were studied at P/L = 1:50, at 310 K in POPC and DMPC/DMPG and at 295 K in the other lipid systems. These results all fit to our spontaneous curvature hypothesis.

Recently, the temperature dependent re-alignment of PGLa in DMPC was studied by ^{19}F-NMR [34]. At low concentration the peptide was found to be in the S-state at all temperatures. At higher concentrations, the orientation of PGLa was markedly temperature dependent. The S-state was found at high temperature, the T-state was observed slightly above the lipid phase transition temperature T_m, and an inserted I-state occurred at temperatures below T_m, followed by an aggregated state at low temperatures when the lipids formed a sub-gel phase. It was thus suggested that the T-state, which was only observed close to T_m, might be due to a partial formation of gel phase for the lipids. If

this was the case for MSI-103, it would explain why the T-state was not found in the unsaturated systems studied here, since the measurements were performed at 30 °C, which is well above T_m of DOPC, POPC and POPG (see Table 2). However, we clearly obtained the T-state in DLPC at 30 °C, which has a T_m of about 0 °C. This observation evidently does not support the hypothesis that the T-state would occur only closely to T_m. Instead, the whole picture could be well rationalized if we assume that the spontaneous curvature of a lipid bilayer changes with temperature (i.e. becomes more negative with increasing temperature), but to our knowledge there is no data to support this idea.

In most of the numerous solid-state NMR studies on the orientation of peptides in membranes, only a single lipid system has been employed, usually DMPC or POPC, sometimes in a mixture with the corresponding PG lipid (see Table 3 in [5]). In a few cases several different lipid systems were used and the effect on orientations studied. For example, the antimicrobial peptide LL-37 was studied by ^{15}N-NMR in DMPC, DMPC/DMPG, POPC and POPC/POPG at P/L = 1:50, and in POPE at P/L = 1:20, at 35 °C or 55 °C, and an S-state was found in all cases [17]. A study of LL-37 in ^{2}H-labeled DMPC and POPC bilayers [70] showed that the peptide was inserted more deeply into DMPC than in POPC. From our results on MSI-103, it is not surprising that the S-state was found in the unsaturated systems, and the deeper insertion into DMPC would fit with our results. The lack of a tilted state may be due to several factors: for example, a higher peptide concentration may be needed for this particular peptide to reach the T-state (i.e. it may have a higher P/L* threshold), or the tilted state found for PGLa and MSI-103 depends on dimerization which is not present in LL-37.

Oriented circular dichroism (OCD) has been used to study the alignment behavior of several peptides in lipid bilayers. (For a recent review see [71].) The method does not give an azimuthal rotation angle, and the tilt angle cannot be obtained directly. Nevertheless, when two different alignment states are known, the OCD spectra can be used to estimate the proportion of each state in a sample [72]. Alamethicin is an extensively studied AMP, which has been shown to form pores according to the barrel-stave model [73,74]. The characteristic S-state and I-state orientations of alamethicin were independently described and could be used as standard states for the OCD analysis. The transitions between these two states have thus been studied by OCD as a function of several factors: peptide concentration, humidity, as well as lipid composition [71]. In particular, plots of the inserted fraction of alamethicin as a function of P/L shows a threshold concentration P/L* above which insertion starts taking place. The value of P/L* is generally higher for measurements performed at higher relative humidity [75–78] and also depends on the temperature [76], thus describing a proper phase diagram. For constant temperature and hydration, the lipid composition was shown to be important. A clear indication of the lipid influence was found by OCD analysis for melittin and alamethicin. In both cases, compared to the P/L* values in PC bilayers, the P/L* increased when PE with the same acyl chains was added, while P/L* decreased when lyso-PC was added [79]. Thus, a clear correlation between lipid curvature and P/L* was implicit [79], fully consistent with our findings here. There was also a distinct effect on P/L* in pure PC lipids depending on the acyl chains [80], in agreement with our interpretation.

The antimicrobial peptide magainin 2 was studied by ^{15}N-NMR in POPC, POPC/POPG, POPE/POPG and POPC/POPG/cholesterol, and an S-state was found in all cases [81]. Also in di-10:0-PC at P/L = 1:50 an S-state was found [69]. Magainin 2 was shown by OCD to insert in saturated DMPC/DMPG bilayers with a P/L* threshold of about 1:30, but it remained surface-bound in unsaturated POPC up to P/L = 1:20 [82]. These results fit very nicely with our present results.

Zervamicin II, another antimicrobial peptide, was studied by ^{15}N-NMR in PC lipids of different lengths, at P/L ratios between 1:100 and 1:200 [83]. The peptide was found in the S-state in di-18:1-PC, di-16:1-PC and di-14:1-PC, while an I-state was seen in di-12:0-PC and di-10:0-PC. This difference was interpreted as an effect of hydrophobic mismatch, but the results also correlate very well with the unsaturation of the lipids and thus with the differences in spontaneous curvature. The temperature at which measurements were done was not stated, but lipids were reported to be in the L_α phase.

Also the membrane-lysing peptide pardaxin was studied with ^{15}N-NMR, and at P/L = 1:50 an S-state was found in POPC, versus an I-state in DMPC [84]. In POPC the orientation was independent of temperature over the range between −10 °C and +20 °C [85]. Also in DMPC/DMPG (3:1) and in DMPC/cholesterol (85:15) an I-state was found [86]. These results agree well with the effect of spontaneous curvature found here. In the presence of cholesterol, on the other hand, pardaxin was seen to insert into the membrane, in contrast to our findings on MSI-103. We note, however, that the cholesterol concentration of 15 mol% was lower than the 20 mol% in our study.

In all of these ^{15}N-NMR studies of α-helical peptides, an approximate helix tilt angle was obtained but no azimuthal rotation angle. In a ^{13}C-NMR study of the β-turn peptide protegrin-1, it was concluded that the peptide was monomeric in DLPC but formed large aggregates in DMPC and POPC [87]. The orientation was not directly measured, but the authors concluded that the monomeric peptide was tilted about 55° in DLPC, corresponding to a T-state, while it formed some kind of membrane-spanning oligomer in the longer lipids, which might be a mismatch effect. Again, these results would also seem to correlate with the relative spontaneous curvatures of the different lipid systems, as DLPC has the highest positive curvature and could accommodate the tilted monomers in the "void space" of its acyl chain region. It will thus be interesting to see whether our hypothesis should hold not only for α-helical peptides but also for other amphiphilic conformations such as β-structures. This, in turn, would imply a marked relevance for membrane-active amphiphilic peptides in general, as most antimicrobial peptides, cell penetrating agents, and fusogenic sequences fall into this category.

In summary, there are not many studies of membrane-active peptides where a systematic variation of the lipid composition has been performed yet. Nevertheless, for those cases where several lipids have been used, there is a clear correlation between the orientation found for the peptide and the spontaneous curvature of the lipid system. Basically, the peptides are seen to insert only in systems with a positive spontaneous curvature. Real biological membranes are complex assemblies of lipids, proteins and other molecules, and it is hard to estimate the spontaneous curvature of such systems. From the present results and previous studies, it seems that peptides are hardly able to insert into membranes composed of POPE/POPG, which are often used to mimic bacterial membranes. A similar observation was recently reported in a ^{19}F-NMR analysis of PGLa and gramicidin S in native biomembranes prepared from bacterial protoplasts and from human erythrocytes [8,9]. The question thus has to remain open, whether the action of antimicrobial peptides is usually more of the carpet type with surface-bound peptides disturbing the membrane, or whether an extremely high local concentration is needed (corresponding to a very high P/L* value) for the peptides to insert and induce a transient instability, or whether a distinct self-assembly and/or conformational change of the peptide occurs that will influence its intrinsic geometry and mode of membrane-interaction.

5. Conclusions

The orientation of a peptide in a membrane depends on many factors, and lipid composition is one of them. Many studies of membrane-active peptides have been performed in model bilayers consisting of only one well-defined lipid species or one particular lipid mixture, hence their conclusions may not be generally applicable to natural systems. Yet, from a biophysical point of view it is essential to understand the detailed molecular mechanisms involved in the lipid–peptide interactions. Therefore membrane-active peptides need to be studied systematically in several lipid systems, using methods like solid-state NMR to obtain detailed

structural information. From a biological point of view it is important to choose lipid systems most closely resembling the biological membrane of interest, when the biological aspects of membrane peptides and proteins are to be interpreted.

In the present study, we find that the antimicrobial peptide MSI-103 has two preferred orientational states under the conditions studied: a surface-bound S-state with a tilt angle τ close to 90°, and an obliquely inserted orientation with τ close to 130°, which we call the T-state. It has been proposed that these two distinct states correspond to monomers and dimers of the peptide, respectively. In some cases intermediate tilt angles are observed, which can be explained by a fast exchange between the S- and the T-state (i.e. when the concentration is close to P/L*). We see a strong correlation between the helix orientation and the spontaneous curvature of the lipid systems, as illustrated in Fig. 6. In unsaturated lipids, or more generally in bilayers with a negative spontaneous curvature, only the S-state is found, even at high peptide concentration. On the other hand, in saturated lipids, and in the presence of lyso-lipids or more generally in bilayers with a positive spontaneous curvature, the T-state is found at higher peptide concentrations.

Other studies of membrane-active peptides have also in some cases found differences in orientation depending on the lipid composition, and all of these results are consistent with the hypothesis presented here. Yet, nobody has previously studied a sufficient number of lipid systems on the same peptide under equivalent conditions, to be able to produce direct evidence of such connection to spontaneous curvature. This simple model proposed here will very likely be a useful help in the interpretation of peptide–lipid interactions.

Acknowledgements

We thank Nathalie Kanithasen for help with synthesis and purification of peptides. This work was supported by the DFG-Center for Functional Nanostructures in Karlsruhe (E1.2).

Appendices A-C. Supplementary data

Supplementary data to this article can be found online at doi:10.1016/j.bbamem.2012.02.027.

References

[1] P. Wadhwani, J. Reichert, J. Bürck, A.S. Ulrich, Antimicrobial and cell penetrating peptides induce lipid vesicle fusion by folding and aggregation, Eur. Biophys. J. 41 (2012) 177–187.
[2] K.A. Brogden, Antimicrobial peptides: pore formers or metabolic inhibitors in bacteria? Nat. Rev. Microbiol. 3 (2005) 238–250.
[3] R.E. Hancock, H.G. Sahl, Antimicrobial and host-defense peptides as new anti-infective therapeutic strategies, Nat. Biotechnol. 24 (2006) 1551–1557.
[4] T. Wieprecht, O. Apostolov, M. Beyermann, J. Seelig, Membrane binding and pore formation of the antibacterial peptide PGLa: thermodynamic and mechanistic aspects, Biochemistry 39 (2000) 442–452.
[5] E. Strandberg, A.S. Ulrich, NMR methods for studying membrane-active antimicrobial peptides, Concepts Magn. Reson. A 23A (2004) 89–120.
[6] A.S. Ulrich, P. Wadhwani, U.H.N. Dürr, S. Afonin, R.W. Glaser, E. Strandberg, P. Tremouilhac, C. Sachse, M. Berditchevskaia, S.L. Grage, Solid-state ^{19}F-nuclear magnetic resonance analysis of membrane-active peptides, in: A. Ramamoorthy (Ed.), NMR Spectroscopy of Biological Solids, CRC Press, Boca Raton, FL, 2006, pp. 215–236.
[7] A.S. Ulrich, Solid state ^{19}F-NMR methods for studying biomembranes, Prog. Nucl. Magn. Reson. Spectrosc. 46 (2005) 1–21.
[8] M. Ieronimo, S. Afonin, K. Koch, M. Berditsch, P. Wadhwani, A.S. Ulrich, ^{19}F NMR analysis of the antimicrobial peptide PGLa bound to native cell membranes from bacterial protoplasts and human erythrocytes, J. Am. Chem. Soc. 132 (2010) 8822–8824.
[9] K. Koch, S. Afonin, M. Ieronimo, M. Berditsch, A.S. Ulrich, Solid-state ^{19}F-NMR of peptides in native membranes, Top. Curr. Chem. 306 (2012) 89–118.
[10] P. Wadhwani, E. Strandberg, Structure analysis of membrane-active peptides using ^{19}F-labeled amino acids and solid-state NMR, in: I. Ojima (Ed.), Fluorine in Medicinal Chemistry and Chemical Biology, Blackwell Publishing, London, 2009, pp. 463–493.
[11] S.L. Grage, J.B. Salgado, U.H.N. Dürr, S. Afonin, R.W. Glaser, A.S. Ulrich, Solid state ^{19}F-NMR of biomembranes, in: S.R. Kiihne, H.J.M. deGroot (Eds.), Perspectives on Solid State NMR in Biology, Kluwer Academic Publishers, Dordrecht/Boston/London, 2001, pp. 83–91.
[12] P. Wadhwani, P. Tremouilhac, E. Strandberg, S. Afonin, S.L. Grage, M. Ieronimo, M. Berditsch, A.S. Ulrich, Using fluorinated amino acids for structure analysis of membrane-active peptides by solid-state ^{19}F-NMR, in: V.A. Soloshonok, K. Mikami, T. Yamazaki, J.T. Welch, J.F. Honek (Eds.), Current Fluoroorganic Chemistry: New Synthetic Directions, Technologies, Materials, and Biological Applications, American Chemical Society, Washington, DC, 2007, pp. 431–446.
[13] R. Heinzmann, S.L. Grage, C. Schalck, J. Burck, Z. Banoczi, O. Toke, A.S. Ulrich, A kinked antimicrobial peptide from *Bombina maxima*. II. Behavior in phospholipid bilayers, Eur. Biophys. J. 40 (2011) 463–470.
[14] J.M. Resende, C.M. Moraes, V.H. Munhoz, C. Aisenbrey, R.M. Verly, P. Bertani, A. Cesar, D. Pilo-Veloso, B. Bechinger, Membrane structure and conformational changes of the antibiotic heterodimeric peptide distinctin by solid-state NMR spectroscopy, Proc. Natl. Acad. Sci. U. S. A. 106 (2009) 16639–16644.
[15] B. Bechinger, M. Zasloff, S.J. Opella, Structure and orientation of the antibiotic peptide magainin in membranes by solid-state nuclear magnetic resonance spectroscopy, Protein Sci. 2 (1993) 2077–2084.
[16] M.S. Balla, J.H. Bowie, F. Separovic, Solid-state NMR study of antimicrobial peptides from Australian frogs in phospholipid membranes, Eur. Biophys. J. (2003).
[17] K.A. Henzler Wildman, D.K. Lee, A. Ramamoorthy, Mechanism of lipid bilayer disruption by the human antimicrobial peptide, LL-37, Biochemistry 42 (2003) 6545–6558.
[18] F.M. Marassi, C. Ma, J.J. Gesell, S.J. Opella, Three-dimensional solid-state NMR spectroscopy is essential for resolution of resonances from in-plane residues in uniformly ^{15}N-labeled helical membrane proteins in oriented lipid bilayers, J. Magn. Reson. 144 (2000) 156–161.
[19] E. Strandberg, P. Wadhwani, P. Tremouilhac, U.H.N. Dürr, A.S. Ulrich, Solid-state NMR analysis of the PGLa peptide orientation in DMPC bilayers: structural fidelity of ^{2}H-labels versus high sensitivity of ^{19}F-NMR, Biophys. J. 90 (2006) 1676–1686.
[20] P. Tremouilhac, E. Strandberg, P. Wadhwani, A.S. Ulrich, Conditions affecting the re-alignment of the antimicrobial peptide PGLa in membranes as monitored by solid state ^{2}H-NMR, Biochim. Biophys. Acta 1758 (2006) 1330–1342.
[21] P. Tremouilhac, E. Strandberg, P. Wadhwani, A.S. Ulrich, Synergistic transmembrane alignment of the antimicrobial heterodimer PGLa/magainin, J. Biol. Chem. 281 (2006) 32089–32094.
[22] E. Strandberg, N. Kanithasen, J. Bürck, P. Wadhwani, D. Tiltak, O. Zwernemann, A.S. Ulrich, Solid state NMR analysis comparing the designer-made antibiotic MSI-103 with its parent peptide PGLa in lipid bilayers, Biochemistry 47 (2008) 2601–2616.
[23] R.W. Glaser, C. Sachse, U.H.N. Dürr, S. Afonin, P. Wadhwani, E. Strandberg, A.S. Ulrich, Concentration-dependent realignment of the antimicrobial peptide PGLa in lipid membranes observed by solid-state ^{19}F-NMR, Biophys. J. 88 (2005) 3392–3397.
[24] R.W. Glaser, C. Sachse, U.H.N. Dürr, P. Wadhwani, A.S. Ulrich, Orientation of the antimicrobial peptide PGLa in lipid membranes determined from ^{19}F-NMR dipolar couplings of 4-CF_3-phenylglycine labels, J. Magn. Reson. 168 (2004) 153–163.
[25] P. Wadhwani, J. Bürck, E. Strandberg, C. Mink, S. Afonin, A.S. Ulrich, Using a sterically restrictive amino acid as a ^{19}F-NMR label to monitor and control peptide aggregation in membranes, J. Am. Chem. Soc. 130 (2008) 16515–16517.
[26] D. Maisch, P. Wadhwani, S. Afonin, C. Böttcher, B. Koksch, A.S. Ulrich, Chemical labeling strategy with (R)- and (S)-trifluoromethylalanine for solid state ^{19}F NMR analysis of peptaibols in membranes, J. Am. Chem. Soc. 131 (2009) 15596–15597.
[27] S. Afonin, U.H.N. Dürr, P. Wadhwani, J.B. Salgado, A.S. Ulrich, Solid state NMR structure analysis of the antimicrobial peptide gramicidin S in lipid membranes: concentration-dependent re-alignment and self-assembly as a β-barrel, Top. Curr. Chem. 273 (2008) 139–154.
[28] J. Salgado, S.L. Grage, L.H. Kondejewski, R.S. Hodges, R.N. McElhaney, A.S. Ulrich, Membrane-bound structure and alignment of the antimicrobial β-sheet peptide gramicidin S derived from angular and distance constraints by solid state ^{19}F-NMR, J. Biomol. NMR 21 (2001) 191–208.
[29] D. Grasnick, U. Sternberg, E. Strandberg, P. Wadhwani, A.S. Ulrich, Irregular structure of the HIV fusion peptide in membranes demonstrated by solid-state NMR and MD simulations, Eur. Biophys. J. 40 (2011) 529–543.
[30] S. Afonin, U.H.N. Dürr, R.W. Glaser, A.S. Ulrich, 'Boomerang'-like insertion of a fusogenic peptide in a lipid membrane revealed by solid-state ^{19}F NMR, Magn. Reson. Chem. 42 (2004) 195–203.
[31] S.L. Grage, S. Afonin, A.S. Ulrich, Dynamic transitions of membrane active peptides, in: A. Giuliani, A.C. Rinaldi (Eds.), Antimicrobial Peptides. Methods and Protocols, Springer, Humana Press, New York, 2010, pp. 183–209.
[32] A. Latal, G. Degovics, R.F. Epand, R.M. Epand, K. Lohner, Structural aspects of the interaction of peptidyl–glycylleucine–carboxyamide, a highly potent antimicrobial peptide from frog skin, with lipids, Eur. J. Biochem. 248 (1997) 938–946.
[33] J. Bürck, S. Roth, P. Wadhwani, S. Afonin, N. Kanithasen, E. Strandberg, A.S. Ulrich, Conformation and membrane orientation of amphiphilic helical peptides by oriented circular dichroism, Biophys. J. 95 (2008) 3872–3881.
[34] S. Afonin, S.L. Grage, M. Ieronimo, P. Wadhwani, A.S. Ulrich, Temperature-dependent transmembrane insertion of the amphiphilic peptide PGLa in lipid bilayers observed by solid state ^{19}F-NMR spectroscopy, J. Am. Chem. Soc. 130 (2008) 16512–16514.
[35] J. Blazyk, R. Wiegand, J. Klein, J. Hammer, R.M. Epand, R.F. Epand, W.L. Maloy, U.P. Kari, A novel linear amphipathic β-sheet cationic antimicrobial peptide with enhanced selectivity for bacterial lipids, J. Biol. Chem. 276 (2001) 27899–27906.
[36] W.L. Maloy, U.P. Kari, Structure-activity studies on magainins and other host-defense peptides, Biopolymers 37 (1995) 105–122.

[37] E. Strandberg, D. Tiltak, M. Ieronimo, N. Kanithasen, P. Wadhwani, A.S. Ulrich, Influence of C-terminal amidation on the antimicrobial and hemolytic activities of cationic α-helical peptides, Pure Appl. Chem. 79 (2007) 717–728.
[38] P.F. Devaux, M. Seigneuret, Specificity of lipid–protein interactions as determined by spectroscopic techniques, Biochim. Biophys. Acta 822 (1985) 63–125.
[39] S.H. Park, A.A. De Angelis, A.A. Nevzorov, C.H. Wu, S.J. Opella, Three-dimensional structure of the transmembrane domain of Vpu from HIV-1 in aligned phospholipid bicelles, Biophys. J. 91 (2006) 3032–3042.
[40] S.H. Park, S.J. Opella, Tilt angle of a trans-membrane helix is determined by hydrophobic mismatch, J. Mol. Biol. 350 (2005) 310–318.
[41] E. Strandberg, S. Özdirekcan, D.T.S. Rijkers, P.C.A. Van der Wel, R.E. Koeppe II, R.M.J. Liskamp, J.A. Killian, Tilt angles of transmembrane model peptides in oriented and non-oriented lipid bilayers as determined by ^{2}H solid state NMR, Biophys. J. 86 (2004) 3709–3721.
[42] S. Özdirekcan, D.T.S. Rijkers, R.M.J. Liskamp, J.A. Killian, Influence of flanking residues on tilt and rotation angles of transmembrane peptides in lipid bilayers. A solid-state ^{2}H NMR study, Biochemistry 44 (2005) 1004–1012.
[43] P.C.A. Van der Wel, E. Strandberg, J.A. Killian, R.E. Koeppe II, Geometry and intrinsic tilt of a tryptophan-anchored transmembrane α-helix determined by ^{2}H NMR, Biophys. J. 83 (2002) 1479–1488.
[44] E. Strandberg, S. Esteban-Martín, J. Salgado, A.S. Ulrich, Orientation and dynamics of peptides in membranes calculated from ^{2}H-NMR data, Biophys. J. 96 (2009) 3223–3232.
[45] D. Marsh, Energetics of hydrophobic matching in lipid–protein interactions, Biophys. J. 94 (2008) 3996–4013.
[46] J.A. Killian, M.J. Taylor, R.E. Koeppe, Orientation of the valine-1 side chain of the gramicidin transmembrane channel and implications for channel functioning. A ^{2}H NMR study, Biochemistry 31 (1992) 11283–11290.
[47] S. Afonin, R.W. Glaser, M. Berditchevskaia, P. Wadhwani, K.H. Guhrs, U. Mollmann, A. Perner, A.S. Ulrich, 4-Fluorophenylglycine as a label for ^{19}F-NMR structure analysis of membrane-associated peptides, Chembiochem 4 (2003) 1151–1163.
[48] R.B. Gennis, Biomembranes. Molecular Structure and Function, Springer-Verlag, New York, 1989.
[49] T. Kobayashi, M. Nishijima, Y. Tamori, S. Nojima, Y. Seyama, T. Yamakawa, Acyl phosphatidylglycerol of *Escherichia coli*, Biochim. Biophys. Acta 620 (1980) 356–363.
[50] A.G. Rietveld, J.A. Killian, W. Dowhan, B. Dekruijff, Polymorphic regulation of membrane phospholipid composition in *Escherichia coli*, J. Biol. Chem. 268 (1993) 12427–12433.
[51] C.R.H. Raetz, Enzymology, genetics, and regulation of membrane phospholipid synthesis in *Escherichia coli*, Microbiol. Rev. 42 (1978) 614–659.
[52] P.F. Devaux, R. Morris, Transmembrane asymmetry and lateral domains in biological membranes, Traffic 5 (2004) 241–246.
[53] J.N. Israelachvili, D.J. Mitchell, B.W. Ninham, Theory of self-assembly of lipid bilayers and vesicles, Biochim. Biophys. Acta 470 (1977) 185–201.
[54] P.R. Cullis, B. de Kruijff, Lipid polymorphism and the functional roles of lipids in biological membranes, Biochim. Biophys. Acta 559 (1979) 399–420.
[55] M.M. Kamal, D. Mills, M. Grzybek, J. Howard, Measurement of the membrane curvature preference of phospholipids reveals only weak coupling between lipid shape and leaflet curvature, Proc. Natl. Acad. Sci. U. S. A. 106 (2009) 22245–22250.
[56] E.E. Kooijman, V. Chupin, N.L. Fuller, M.M. Kozlov, B. de Kruijff, K.N. Burger, P.R. Rand, Spontaneous curvature of phosphatidic acid and lysophosphatidic acid, Biochemistry 44 (2005) 2097–2102.
[57] N. Fuller, C.R. Benatti, R.P. Rand, Curvature and bending constants for phosphatidylserine-containing membranes, Biophys. J. 85 (2003) 1667–1674.
[58] S. Leikin, M.M. Kozlov, N.L. Fuller, R.P. Rand, Measured effects of diacylglycerol on structural and elastic properties of phospholipid membranes, Biophys. J. 71 (1996) 2623–2632.
[59] R.P. Rand, N.L. Fuller, S.M. Gruner, V.A. Parsegian, Membrane curvature, lipid segregation, and structural transitions for phospholipids under dual-solvent stress, Biochemistry 29 (1990) 76–87.
[60] N. Fuller, R.P. Rand, The influence of lysolipids on the spontaneous curvature and bending elasticity of phospholipid membranes, Biophys. J. 81 (2001) 243–254.
[61] J.A. Szule, N.L. Fuller, R.P. Rand, The effects of acyl chain length and saturation of diacylglycerols and phosphatidylcholines on membrane monolayer curvature, Biophys. J. 83 (2002) 977–984.
[62] D. Marsh, Lateral pressure profile, spontaneous curvature frustration, and the incorporation and conformation of proteins in membranes, Biophys. J. 93 (2007) 3884–3899.
[63] S.W. Hui, A. Sen, Effects of lipid packing on polymorphic phase behavior and membrane properties, Proc. Natl. Acad. Sci. U. S. A. 86 (1989) 5825–5829.
[64] S.H. Alley, O. Ces, M. Barahona, R.H. Templer, X-ray diffraction measurement of the monolayer spontaneous curvature of dioleoylphosphatidylglycerol, Chem. Phys. Lipids 154 (2008) 64–67.
[65] R.S. Cantor, Lateral pressures in cell membranes: a mechanism for modulation of protein function, J. Phys. Chem. B 101 (1997) 1723–1725.
[66] R.S. Cantor, The lateral pressure profile in membranes: a physical mechanism of general anesthesia, Biochemistry 36 (1997) 2339–2344.
[67] K. Shintou, M. Nakano, T. Kamo, Y. Kuroda, T. Handa, Interaction of an amphipathic peptide with phosphatidycholine/phosphatidylethanolamine mixed membranes, Biophys. J. 93 (2007) 3900–3906.
[68] M. Nakano, T. Kamo, Y. Kuroda, T. Handa, Effects of an amphipathic alpha-helical peptide on lateral pressure and water penetration in phosphatidylcholine and monoolein mixed membranes, J. Phys. Chem. B 110 (2006) 24987–24992.
[69] E.S. Salnikov, B. Bechinger, Lipid-controlled peptide topology and interactions in bilayers: structural insights into the synergistic enhancement of the antimicrobial activities of PGLa and magainin 2, Biophys. J. 100 (2011) 1473–1480.
[70] K.A. Henzler-Wildman, G.V. Martinez, M.F. Brown, A. Ramamoorthy, Perturbation of the hydrophobic core of lipid bilayers by the human antimicrobial peptide LL-37, Biochemistry 43 (2004) 8459–8469.
[71] H.W. Huang, Molecular mechanism of antimicrobial peptides: the origin of cooperativity, Biochim. Biophys. Acta 1758 (2006) 1292–1302.
[72] Y. Wu, H.W. Huang, G.A. Olah, Method of oriented circular dichroism, Biophys. J. 57 (1990) 797–806.
[73] R.O. Fox Jr., F.M. Richards, A voltage-gated ion channel model inferred from the crystal structure of alamethicin at 1.5-A resolution, Nature 300 (1982) 325–330.
[74] B. Leitgeb, A. Szekeres, L. Manczinger, C. Vagvolgyi, L. Kredics, The history of alamethicin: a review of the most extensively studied peptaibol, Chem. Biodivers. 4 (2007) 1027–1051.
[75] W.T. Heller, K. He, S.J. Ludtke, T.A. Harroun, H.W. Huang, Effect of changing the size of lipid headgroup on peptide insertion into membranes, Biophys. J. 73 (1997) 239–244.
[76] L. Yang, T.A. Harroun, T.M. Weiss, L. Ding, H.W. Huang, Barrel-stave model or toroidal model? A case study on melittin pores, Biophys. J. 81 (2001) 1475–1485.
[77] H.W. Huang, Y. Wu, Lipid–alamethicin interactions influence alamethicin orientation, Biophys. J. 60 (1991) 1079–1087.
[78] W.T. Heller, A.J. Waring, R.I. Lehrer, H.W. Huang, Multiple states of β-sheet peptide protegrin in lipid bilayers, Biochemistry 37 (1998) 17331–17338.
[79] M.T. Lee, W.C. Hung, F.Y. Chen, H.W. Huang, Many-body effect of antimicrobial peptides: on the correlation between lipid's spontaneous curvature and pore formation, Biophys. J. 89 (2005) 4006–4016.
[80] M.T. Lee, F.Y. Chen, H.W. Huang, Energetics of pore formation induced by membrane active peptides, Biochemistry 43 (2004) 3590–3599.
[81] B. Bechinger, M. Zasloff, S.J. Opella, Structure and interactions of magainin antibiotic peptides in lipid bilayers: a solid-state nuclear magnetic resonance investigation, Biophys. J. 62 (1992) 12–14.
[82] S.J. Ludtke, K. He, W.T. Heller, T.A. Harroun, L. Yang, H.W. Huang, Membrane pores induced by magainin, Biochemistry 35 (1996) 13723–13728.
[83] B. Bechinger, D.A. Skladnev, A. Ogrel, X. Li, E.V. Rogozhkina, T.V. Ovchinnikova, J.D.J. O'Neil, J. Raap, ^{15}N and ^{31}P solid-state NMR investigations on the orientation of zervamicin II and alamethicin in phosphatidylcholine membranes, Biochemistry 40 (2001) 9428–9437.
[84] K.J. Hallock, D.K. Lee, J. Omnaas, H.I. Mosberg, A. Ramamoorthy, Membrane composition determines pardaxin's mechanism of lipid bilayer disruption, Biophys. J. 83 (2002) 1004–1013.
[85] F. Porcelli, B. Buck, D.K. Lee, K.J. Hallock, A. Ramamoorthy, G. Veglia, Structure and orientation of pardaxin determined by NMR experiments in model membranes, J. Biol. Chem. 279 (2004) 45815–45823.
[86] A. Ramamoorthy, D.K. Lee, T. Narasimhaswamy, R.P.R. Nanga, Cholesterol reduces pardaxin's dynamics-a barrel-stave mechanism of membrane disruption investigated by solid-state NMR, Biochim. Biophys. Acta 1798 (2010) 223–227.
[87] J.J. Buffy, A.J. Waring, R.I. Lehrer, M. Hong, Immobilization and aggregation of the antimicrobial peptide protegrin-1 in lipid bilayers investigated by solid-state NMR, Biochemistry 42 (2003) 13725–13734.
[88] R. Koynova, M. Caffrey, Phases and phase transitions of the phosphatidylcholines, Biochim. Biophys. Acta 1376 (1998) 91–145.
[89] Y.P. Zhang, R.N.A.H. Lewis, R.N. McElhaney, Calorimetric and spectroscopic studies of the thermotropic phase behavior of the n-saturated 1,2-diacylphosphatidylglycerols, Biophys. J. 72 (1997) 779–793.
[90] R. Koynova, M. Caffrey, Phases and phase transitions of the hydrated phosphatidylethanolamines, Chem. Phys. Lipids 69 (1994) 1–34.
[91] F. Borle, J. Seelig, Ca^{2+} binding to phosphatidylglycerol bilayers as studied by differential scanning calorimetry and ^{2}H- and ^{31}P-nuclear magnetic resonance, Chem. Phys. Lipids 36 (1985) 263–283.